CONTROL OF MORPHOLOGY AND LUMINESCENSE OF NANOSTRUCTURED ZnO LAYERS FOR LASING APPLICATIONS

Alexandru Burlacu

Ghitu Institute of Electronic Engineering and Nanotechnology, Academy of Sciences of Moldova, str. Academiei 3/3, Chisinau, MD-2028 Republic of Moldova

E-mail: alexandru.burlacu@asm.md

(Received December 2, 2016)

Abstract

A comparative analysis of various technological methods for the preparation of nanostructured ZnO films is performed in this work to identify technologies suitable for the development of laser structures. It is shown that arrays of nanorods with a regular hexagonal geometry are readily produced by low-pressure chemical vapor deposition (CVD), chemical bath deposition (CBD), and electrochemical depositions (ECD) and these nanorods can play the role of resonators for guided modes. Irregular nanostructured layers with strong light scattering properties can be prepared by metal-organic chemical vapor deposition (MOCVD), aerosol spray pyrolysis, and by thermal treatment of ZnSe crystals. As concerns the optical quality necessary for stimulated emission and optical gain, low-pressure CVD and MOCVD are most suitable, while CBD and ECD can hardly provide the required quality for lasing action.

1. Introduction

There has been a steady increasing interest in optoelectronic applications of zinc oxide in the last decades [1–11] due to excellent semiconductor properties of this material, such as high electron mobility and thermal conductivity, good optical transparency, large bandgap (3.36 eV at room temperature), high exciton binding energy (60 meV), high optical gain, (320 cm^{-1} at room temperature), high damage threshold under strong excitations, and high resistance against radiation. These optoelectronic applications include photovoltaic cells, light emitting diodes, and lasers, detectors among others.

Another specific property of ZnO, which results from multiple changes in the growth directions of the wurtzite structure and high ionicity of polar surfaces [12, 13], is that it provides conditions for obtaining a large diversity of micro/nanostructures, such as nanowires, nanobelts, nanorings, nanospirals/nanobows, nanocombs, etc., many of which are suitable for designing lasers.

Therefore, nanostructured ZnO films produced by various technological methods provide conditions for lasing effects with different laser mode structures due to different resonator types, provided that the applied technologies ensure high optical quality of films in terms of optical gain, and high figure of merit of the produced resonators.

The goal of this paper is to perform a comparative analysis of the effect of technological conditions applied during the growth of nanostructured ZnO films by various technological

methods upon the morphology and luminescence properties of the produced films and identify which of them are most suitable for developing lasers.

2. Sample preparation and experimental details

Nanostructured ZnO films were produced by various technologies. Metal organic chemical vapor deposition (MOCVD) was performed in a horizontal double furnace set-up consisting of a source furnace and a main furnace as described elsewhere [14], with a zinc acetylacetonate material introduced into the source furnace. The vapors were transported into the main furnace by an Ar gas flow which was mixed with another flow of Ar and O_2 gases at the entrance of the main furnace. The morphology of ZnO structures produced by this method was determined by the ratio of the gas flow rates.

With chemical vapor deposition (CVD) procedure, ZnO nanowire films were grown on Si (100) substrates at a low pressure (a level of 5 Torr) in a two-zone quartz flow reactor [15, 16] with metallic zinc of high purity (99.999%) and an oxygen–argon mixture (15 vol % of oxygen) as starting reactants. In the first zone, zinc was evaporated; in the second zone, zinc vapors interacted with oxygen. An oxygen–argon mixture was fed to the reactor. The synthesis was conducted on substrates located in the second zone at different distances from the zinc source. ZnO nanowires were synthesized with high yield by controlling the flow rates and partial pressures of oxygen, argon, and zinc vapor. Growth of vertical nanowires started for a certain critical ratio of oxygen/zinc vapors. The shape and size of the ZnO nanowires/nanorods were found to depend on the position of the substrate in the growth zone.

With chemical bath deposition (CBD) method, the substrates were immersed in an aqueous solution bath comprising a mixture of saturated $ZnCl_2$ and concentrated NH_4OH [14, 17].

The reactions of the formation of complex Zn ions and their interaction with NH_4OH are as follows:

$$ZnCl_2{*}2H_2O+4H_2O \leftrightarrow Zn(H_2O)_6^{2+} + 2Cl^-$$
$$Zn(H_2O)_6^{2+} + 2NH_4OH \leftrightarrow Zn(OH)_2\downarrow + 2NH_4^+ + 6H_2O$$
$$Zn(OH)_2 + 4NH_4OH \leftrightarrow Zn(NH_3)_4^{2+} + 2OH^- + 4H_2O$$
$$Zn(NH_3)_4^{2+} + 2OH^- \leftrightarrow Zn(OH)_2\downarrow + 4NH_3\uparrow$$

The substrate with the deposited $Zn(OH)_2$ is calcinated at 250–300^{o}C for 2 h. ZnO nanorods are formed as a result of the reaction:

$$Zn(OH)_2 \rightarrow ZnO + H_2O.$$

Quasi-continuous and nanostructured ZnO layers were obtained by electrochemical deposition (ECD) using a zinc nitrate ($Zn(NO_3)_2$) solution with a concentration of 0.05–20 mM and hydrogen peroxide (H_2O_2) with a concentration of 0.1 M in an electrochemical cell with three electrodes: a metallic zinc or silicon working electrode, an Ag/AgCl reference electrode, and a platinum counter electrode. Aluminum nitrate ($Al(NO_3)_3$) was used for *n*-type doping. The following reactions occur with application of potential at the cathode:

$$NO_3^- + 2\ e^- + H_2O \rightarrow 2\ OH^- + NO_2^-$$
$$H_2O_2 + 2\ e^- \rightarrow 2\ OH^-$$
$$Zn^{2+} + 2\ OH^- \rightarrow Zn(OH)_2$$
$$Zn(OH)_2 \rightarrow ZnO + H_2O.$$

The conversion of zinc hydroxide to zinc oxide, which is deposited on the cathode (substrate), occurs at temperatures above 60°C.

Non-doped and In+N co-doped ZnO films were also prepared by aerosol spray pyrolysis with a special injector under the pressure of an oxygen flow with acetate dihydrate ($Zn(CH_3COO)_2{\cdot}2H_2O$) dissolved in ethylic alcohol. Doping with indium was performed by adding an indium nitrate ($In(NO_3)_3$) solution; doping with nitrogen was achieved by dissolution of ammonium acetate (CH_3COONH_4) stabilized by diethanolamine ($C_4H_{11}NO_2$).

Apart from that, a nanostructured ZnO material was prepared from bulk ZnSe single crystals by their transformation into ZnO by thermal treatment in oxygen ambient at different temperatures in a range of 600–800°C for 1 h.

The morphology and chemical composition microanalysis of samples were studied using a VEGA TESCAN TS 5130MM scanning electron microscope (SEM) equipped with an Oxford Instruments INCA energy dispersive X-ray (EDX) system.

The continuous wave (cw) photoluminescence (PL) was excited by the 351.1-nm line of an Ar^+ SpectraPhysics laser and analyzed with a double spectrometer providing a spectral resolution better than 0.5 meV. The samples were mounted on the cold station of a LTS-22-C-330 optical cryogenic system.

The lasing characteristics of the produced ZnO structures were measured at 10 K in a He-flow cryostat under the pumping by the third harmonic of a Q-switched Nd:YAG laser (355 nm, 10 ns, 10 Hz). The spectra were recorded by a CCD matrix covering a wavelength interval of 40 nm with the dispersion of about 0.04 nm/px.

3. Results and discussion

The MOCVD process usually produces a ZnO film consisting of nanorods with the morphology illustrated in Fig. 1a. The nanorods are arrow-headed with a mean diameter of 200–400 nm. On the other hand, hexagonal ZnO nanorods with a narrow size distribution centered at a diameter of 300 nm are produced with low pressure CVD growth as deduced from analysis of the SEM image in Fig. 1b. The array of nanorods is highly oriented perpendicular to the substrate surface. Arrays of hexagonal ZnO nanorods are also produced by CBD (Fig. 1c) and ECD (Fig. 1d) technologies. A film with a more complex structure consisting of large building blocks, which are nanostructured in turn, is usually produced by aerosol spray pyrolysis as shown in Fig. 1e. As mentioned above, a nanostructured ZnO material with the morphology illustrated in Fig. 1f is obtained by annealing bulk ZnSe single crystals in oxygen ambient.

Analysis of these morphologies in the context of possible laser resonators suggests that arrays of hexagonal nanorods shown in Figs. 1b–1d could sustain laser modes inherent in classical resonators, such as Fabry–Perot (FP) cavities satisfying the following relation [18]:

$$\Delta\lambda = \frac{1}{L}\left[\frac{\lambda^2}{2}\left(n - \lambda\frac{dn}{d\lambda}\right)^{-1}\right]$$

where $\Delta\lambda$ is the wavelength difference for two neighboring modes, L is the resonator length (nanorod length in our case), and n is the refraction index of ZnO, or guided modes resulting from solving the Helmholtz equation for the magnetic field eigenmodes **H**(x,y) and eigenvalues $n_{eff}k_0=\beta$:

$$\nabla\times(\nabla\times H) - n_{eff}^2 k_0^2 H = 0$$

where n_{eff} is the effective refractive index, k_0 is the vacuum wave vector, and β is the propagation constant [19]. On the other hand, the films with morphologies shown in Figs. 1a, 1e, and 1f can most probably sustain random lasing.

Conventional lasing due to FP cavities is unlikely to occur in ZnO nanorods illustrated in Fig. 1a due to the sharp top surface of the ZnO nanorods with large optical loss and an insufficient optical gain in short nanorod with a length of about 1 μm. The arrow-headed ZnO nanorods are not expected to support guided lasing modes either because of their geometrical shape and the wavy form of their surface, which leads to significant light scattering and large optical losses [20]. On the other hand, a random laser does not require a regular cavity; instead, it depends on the scattering properties of the material. It is also hardly expected to find classical regular resonators in layers with the morphology shown in Fig. 1e. On the other hand, strong light scattering is readily provided by this morphology, which is a mandatory condition for random lasing. Conditions for random lasing are most probably fulfilled also in structures produced by annealing of bulk single crystalline ZnSe, which leads to the formation of a uniform nanostructured material with the mean grain size of 100–200 nm as shown in Fig. 1f [21]. Therefore, random laser action is possible in all types of ZnO layers with the morphology shown in Figs. 1a, 1e, and 1f.

In nanorods with a regular hexagonal structure, guided modes can easily propagate and the mode structure can be controlled by changing the geometrical parameters of nanorods as demonstrated in Fig. 2 for ZnO films produced by low-pressure CVD. The size of nanowire/nanorods produced by this technology was found to depend on the O/Zn precursor ratio during growth, which in turn is determined by the position of the substrate in the growth zone [22]. Figure 2a shows that high densities of nanorods with a diameter of 300 nm grow over the ZnO seed layer on a Si substrate positioned at the entrance of the growth zone (higher O/Zn ratio). On the other hand, ZnO nanowires with a diameter of 50–100 nm grow on substrates placed at the exit of the zone (lower O/Zn ratio). The average length of the nanorods/nanowires is about 5 μm.

The morphology of ZnO films produced by ECD can also be controlled by the technological conditions as shown in Fig. 3. Particularly, the density of ZnO nanorods on the substrate depends on the supersaturation level with precursors and on the rates of their refreshing. At high supersaturation levels, a high density of nanorods is produced, which coalesce to form a quasi-continuous film (Fig. 3b). The shapes and sizes of nanorods are also affected by the voltage applied during ECD. Hexagonal nanorods are obtained at an applied voltage of 1.7 V with respect to the reference electrode (Fig. 3a), while arrow-headed nanorods similar to those grown by MOCVD are produced at an applied voltage of 1.8 V (Fig. 3c).

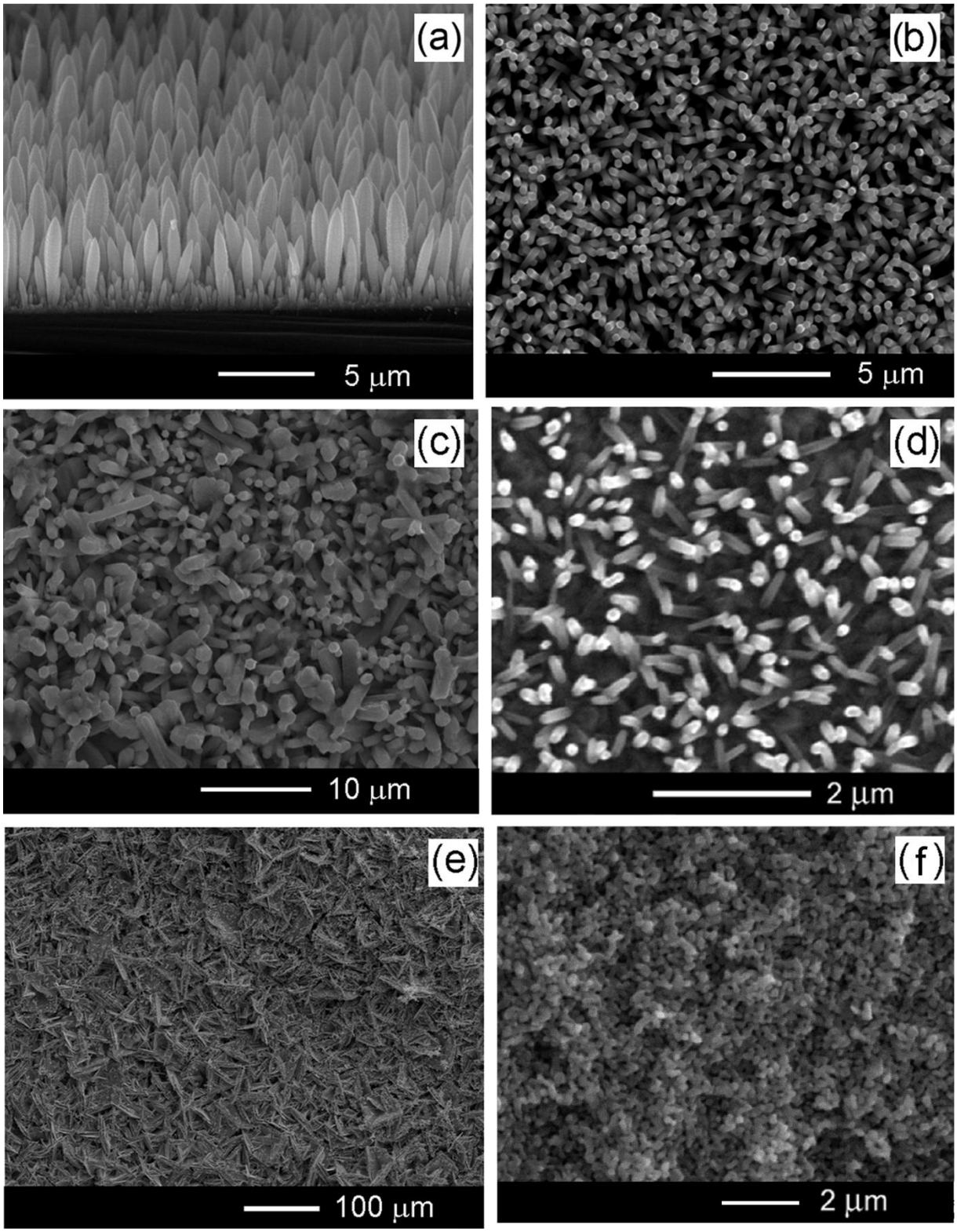

Fig. 1. SEM images of ZnO films produced by various technologies: (a) MOCVD, (b) low-pressure CVD, (c) CBD, (d) ECD, (e) aerosol spray pyrolysis, and (f) thermal treatment of bulk ZnSe.

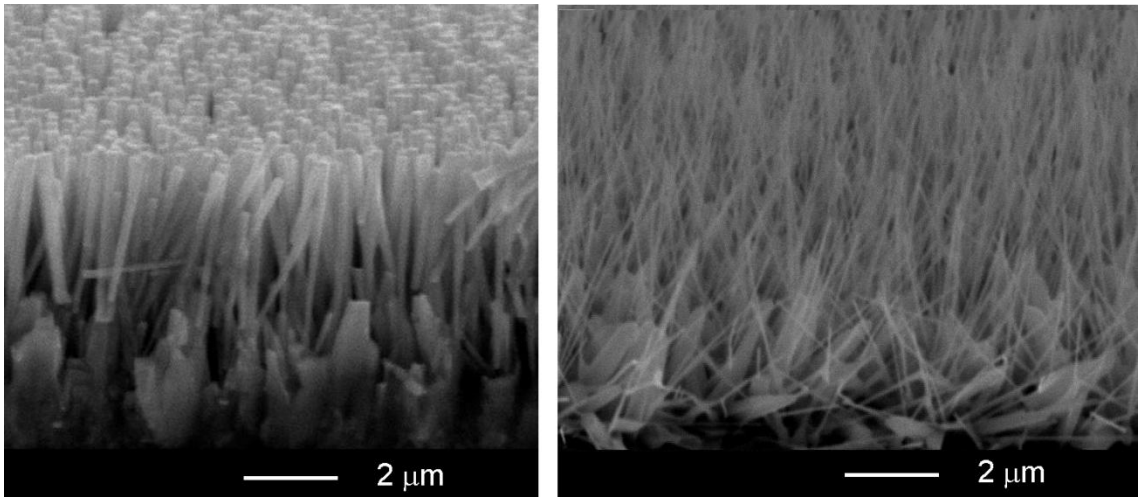

Fig. 2. Tilted SEM view of ZnO nanorods produced by low-pressure CVD with (left) a high and (right) low O/Zn ratio.

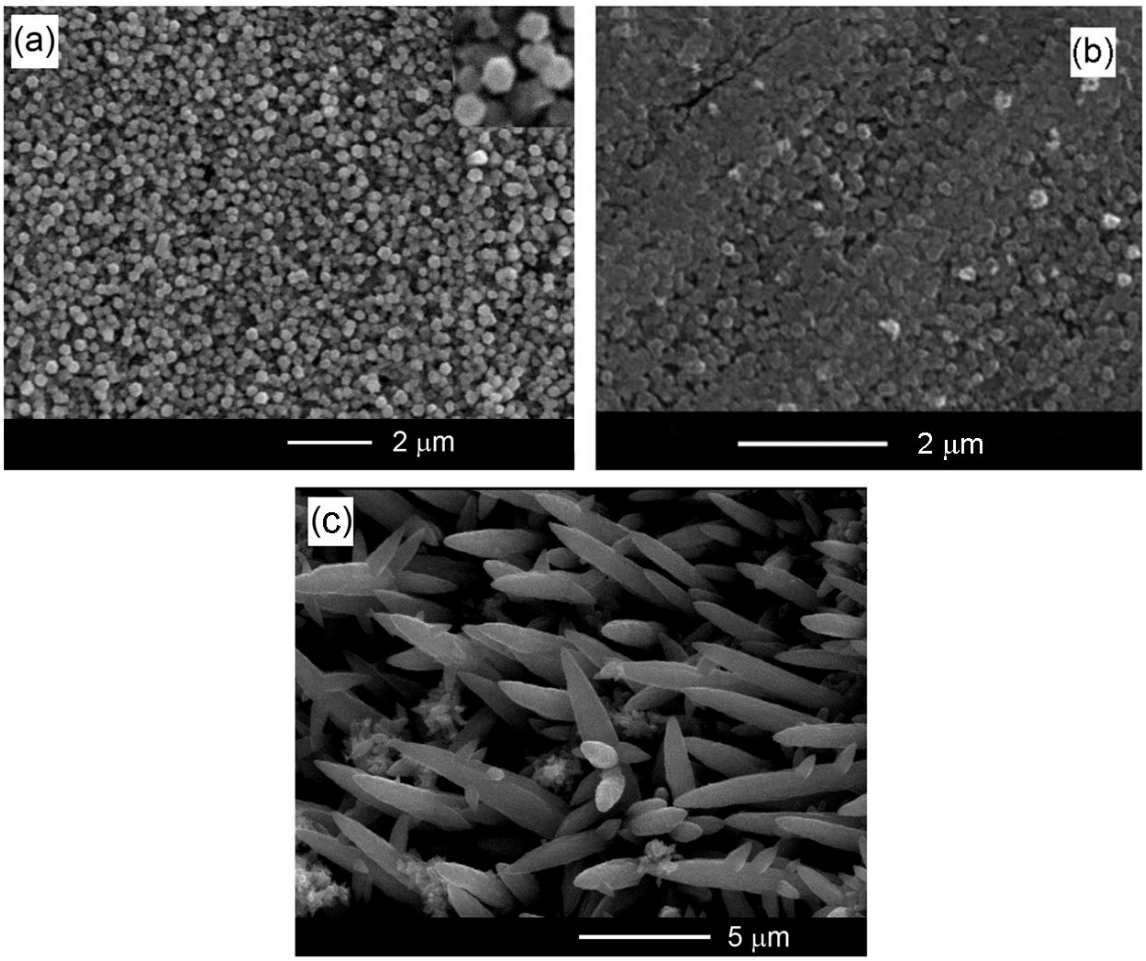

Fig. 3. SEM view of ZnO films produced by ECD with an applied voltage of (a, b) 1.7 and (c) 1.8 V (Ag/AgCl). The concentration of precursors is moderate in (a) and (c) and high in (b).

Apart from high figure of merit resonators, high optical quality of ZnO structures is necessary to provide stimulated emission and laser action. The cw PL characterization revealed the high optical quality of the ZnO structures produced by MOCVD (Fig. 4a) and low-pressure CVD (Fig. 4b). The PL spectrum is dominated by the recombination of donor bound excitons D^0X with phonon replica, along with free exciton FX emission and a band due to the donor acceptor pair recombination DA, the D^0X luminescence in films grown by low-pressure CVD being determined by the I_1, I_4, and I_6 lines [23]. The intensity of the DA luminescence is more than two orders of magnitude lower than the D^0X luminescence. The samples grown by aerosol spray pyrolysis and those produced by thermal treatment of bulk ZnSe also exhibit fairly high optical quality, the PL spectrum being dominated by the recombination of D^0X excitons in the case of the material produced from ZnSe crystals (Fig. 4f) and by the recombination of acceptor-bound excitons A^0X in films prepared by aerosol spray pyrolysis and co-doped by In and N (Fig. 4e).

The samples prepared by the CBD and ECD methods exhibit luminescence properties (Figs. 4c and 4d) different from those of the samples prepared by MOCVD and low-pressure CVD. The low-temperature luminescence intensity in these samples is three orders of magnitude lower, and the PL intensity decreases as little as by a factor of 5 with an increase in temperature to 300 K (not shown here), as compared to the three orders of magnitude decrease in the PL intensity with the same temperature increase in the samples prepared by MOCVD and low-pressure CVD. This observation is indicative of the different natures of electronic transitions responsible for near-band-edge luminescence in the samples prepared by MOCVD or low-pressure CVD on the one side and those prepared by CBD or ECD on the other side. A characteristic feature of the near-bandgap PL band in the samples prepared by CBD and ECD is the broadening towards the Stokes part of the emission. It has been previously shown that the broadening of the PL band involved can be accounted for by the broadening of the band edges due to the potential fluctuations induced by the high concentration of intrinsic defects or impurities [24, 25], and this broadening is a measure of sample doping with impurities.

Apart from the control of morphology by adjusting the technological parameters in the ECD process, the electrical parameters of the deposited films can be controlled by doping with donor impurities, for instance, with aluminum, as described above. The degree of doping with Al, and accordingly the electron concentration, can be monitored by investigating the width of the PL band. Figure 5a presents PL spectra of ZnO films doped with Al from solutions with various concentration of aluminum nitrate (increasing from 1 to 4). The width of the PL band increases from 28 to 155 meV with increasing degree of doping. By using the previously determined dependence of the PL band width on the free electron concentration in ZnO films [26] as a calibration curve, one can estimate that the electron concentration increases from 1.2×10^{19} cm^{-3} in sample #1 to 2.7×10^{20} cm^{-3} in sample #4.

Electrical parameters of the deposited films can also be controlled by doping in an aerosol spray pyrolysis process. The PL spectra presented in Fig. 5b suggest that p-type conductivity can be obtained in ZnO films doped with nitrogen as described above. It is evident that the PL spectrum of a specially undoped sample is dominated by the luminescence at 3.360 eV coming from the recombination of excitons bound to a residual donor impurity, while the spectrum of the sample doped with N is dominated by a PL band at 3.349 eV related to the recombination of acceptor bound excitons [1], most probably of excitons bound to the N acceptor. This assumption was also confirmed by thermoelectric voltage experiments. The possibilities of obtaining films with *p*-type conductivity are especially important for the development of an electrically pumped laser.

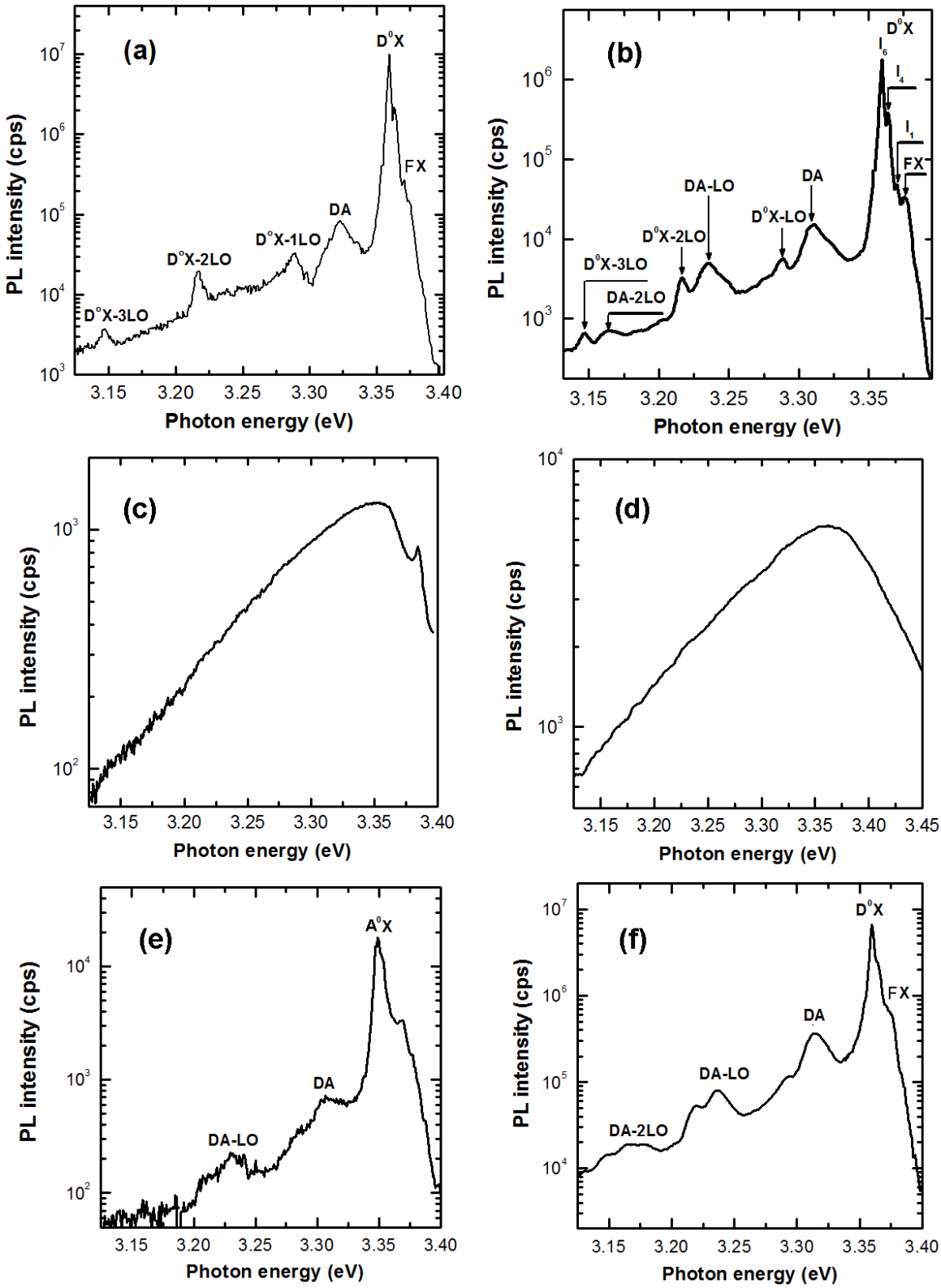

Fig. 4. Typical cw PL spectrum of the ZnO material produced by (a) MOCVD, (b) low-pressure CVD, (c) CBD, (d) ECD, (e) aerosol spray pyrolysis, and (f) thermal treatment of bulk ZnSe. The spectra are measured at T = 10 K.

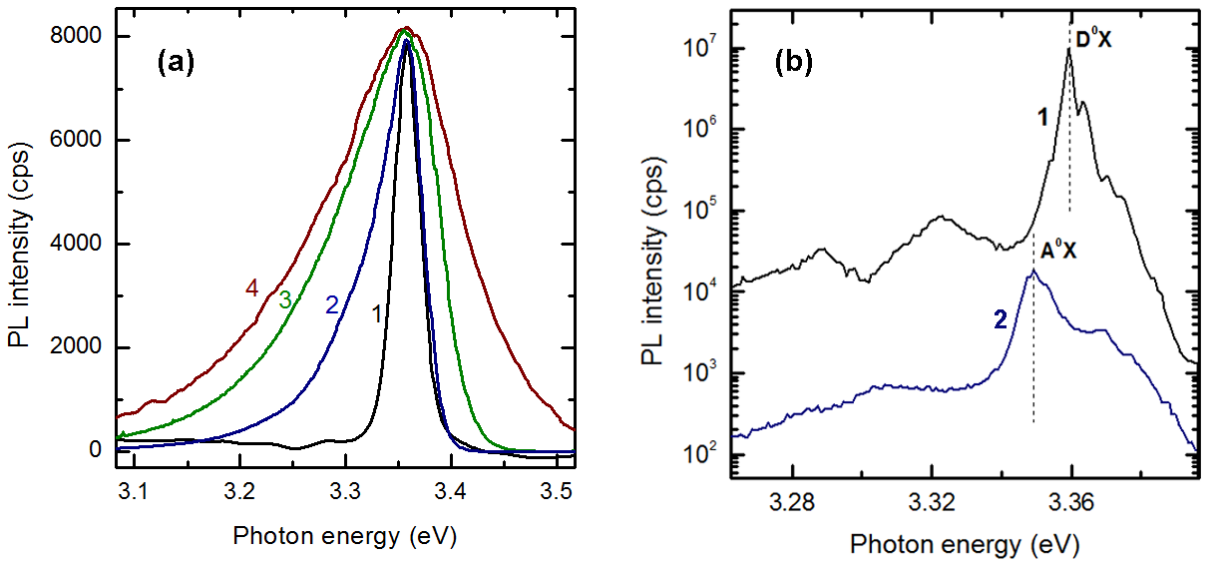

Fig. 5. (a) PL spectra measured at 10 K for ZnO films doped with Al in the ECD process (degree of doping increases from *1* to *4*). (b) PL spectra measured at 10 K for (*1*) the undoped sample and (*2*) for the N-doped sample in the aerosol spray pyrolysis process.

Analysis of PL properties suggests that the films produced by MOCVD and low-pressure CVD should be suitable for the development of lasers, while the optical quality of films prepared by CBD and ECD could be insufficiently high for sustaining stimulated emission and laser action. To verify this issue, the emission spectra of films composed of nanorod arrays with nearly identical morphology and geometrical parameters (as shown in Fig. 6), yet prepared by different methods (by low-pressure CVD and ECD in this case) were studied under pulsed optical pumping under identical conditions. In both cases, the samples have the form of arrays of nanorods with a diameter of about 300 nm and a length of 4–5 μm.

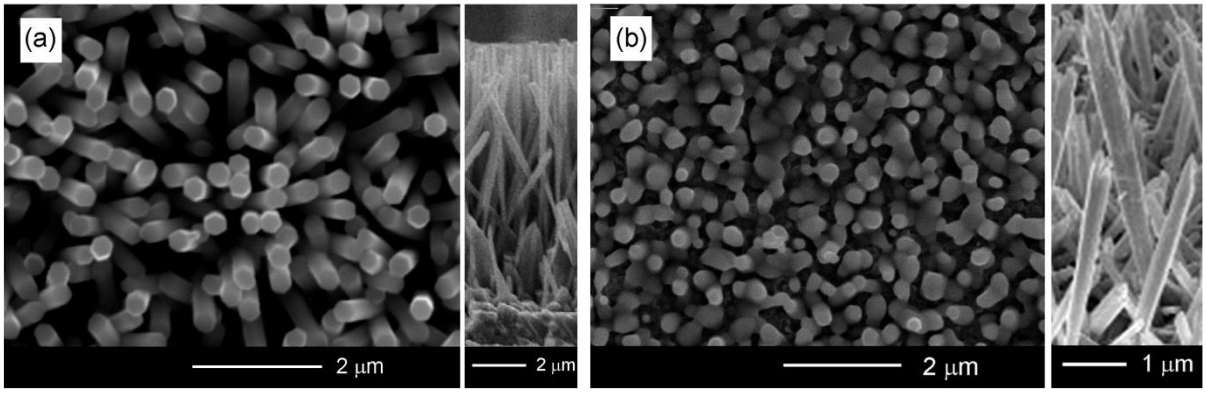

Fig. 6. Top-view and cross-section SEM images of ZnO nanorod films prepared by (a) low-pressure CVD and (b) ECD technologies.

Figure 7a presents the emission spectra of an ensemble of ZnO nanorods with morphology illustrated in Fig. 6a under excitation with a laser spot of 0.2 mm^2. The spectra are

excited by 10-ns laser pulses at a low temperature (10 K) and integrated over 200 pulses. At an excitation power of about 0.2 MW/cm^2, spontaneous emission of about 3.35–3.36 eV is observed. As the pump power increases, the luminescence broadens and undergoes a red shift with increasing intensity. When the power exceeds 0.25 MW/cm^2, additional narrow peaks emerge in the lower energy region. These peaks dramatically increase with a further increase in the pump power. A narrow linewidth (4–5 meV) and a rapid increase in the emission intensities of the peaks indicate that lasing occurs. The observed peaks represent a superposition of lasing modes from different nanorods [20]. In contrast to this, the emission spectrum of the nanorod ensemble grown by ECD with morphology illustrated in Fig. 6b does not change significantly with increasing excitation power density. No narrow emission peaks emerge in the spectrum even at an excitation power density of 3 MW/cm^2; only a broad emission band related to spontaneous emission is observed. With an increase in the excitation power density above 3 MW/cm^2, the sample is damaged without attaining laser action. Therefore, one can conclude that the optical quality of films prepared by ECD in not satisfactory for lasing.

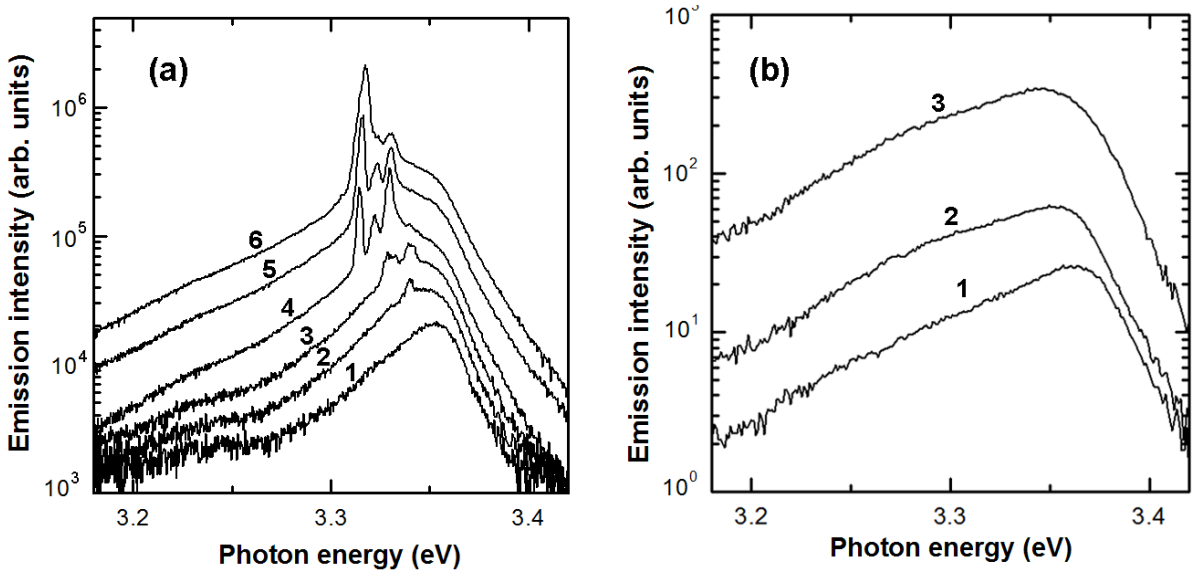

Fig. 7. (a) Lasing in an ensemble of nanorods prepared by low-pressure CVD, as measured at different excitation power densities: (*1*) 200, (*2*) 250, (*3*) 350, (*4*) 500, (*5*) 1500, and (*6*) 2750 kW/cm^2.
(b) Emission spectra of the nanorod array prepared by ECD, as measured at excitation power densities of (*1*) 200, (*2*) 500, and (*3*) 3000 kW/cm^2.

4. Conclusions

This study has shown possibilities of various technological methods to control the morphology and the optical quality of the produced nanostructured ZnO films in view of their implementation in lasers. Investigations of morphologies and emission properties under cw and high-density nanosecond pulsed excitation have shown that low-pressure CVD technologies are most suitable for producing lasing structures with regular resonators sustaining guided modes, while MOCVD, aerosol spray pyrolysis, and thermal treatment of ZnSe crystals produce irregular nanostructures with strong light scattering and high optical quality for random lasers. Wet technologies, such as CBD and ECD, provide the preparation of nanorod arrays which could play

the role of resonators for guided modes; however, procedures should be developed for improving the optical quality to achieve stimulated emission and provide an optical gain for laser action.

References

[1] U. Ozgur, Ya. I Alivov, C. Liu, A. Teke, M.A. Reshchikov, S. Dogan, V. Avrutin, S.J. Cho, and H. Morkoc, J. Appl. Phys., 98, 041301, (2005).
[2] C. Klingshirn, Phys. Stat. Sol. B, 244, 3027, (2007).
[3] H. Morkoc, and U. Ozgur, Zinc Oxide: Fundamentals, Materials and Device Technology, John Wiley & Sons, Weinheim, 2009.
[4] C. F. Klingshirn, B. K. Meyer, A. Waag, A. Hoffmann, J. Geurts, Zinc Oxide: From Fundamental Properties Towards Novel Applications, Springer, Berlin Heidelberg, 2010.
[5] X. W. Sun, and Y. Yang, Zinc Oxide Nanostructures and Their Applications, Pan Stanford Publishing, Boca Raton, 2011.
[6] Ed. C. W. Litton, D.C. Reynolds, and T.C. Collins, Zinc Oxide Materials for Electronic and Optoelectronic Device Applications, John Wiley & Sons, Chichester, 2011.
[7] Ed. C. Jagadish, and S. Pearton, Zinc Oxide Bulk, Thin Films and Nanostructures: Processing, Properties, and Applications, Elsevier, Oxford Kidlington, 2006.
[8] S. J. Pearton, GaN and ZnO-Based Materials and Devices, Springer,Berlin Heidelberg, 2012.
[9] G. -C. Yi, Semiconductor Nanostructures for Optoelectronic Devices: Processing, Characterization and Applications, Springer, Berlin Heidelberg, 2012.
[10] T. Yao and S.-K. Hong, Oxide and Nitride Semiconductors: Processing, Properties, and Applications, Springer, Berlin Heidelberg, 2009.
[11] Z. C. Feng, Handbook of Zinc Oxide and Related Materials, CRC Press, Boca Raton, 2012.
[12] Z. L. Wang, X. Y. Kong, Y. Ding, P. Gao, W.L. Hughes, R. Yang, and Y. Zhang, Adv. Funct. Mater. 14, 943, (2004).
[13] Z. L. Wang, J. Phys.: Condens. Matter, 16, R829, (2004).
[14] A. Burlacu, V. V. Ursaki, V. A. Skuratov, D. Lincot, T. Pauporte, H. Elbelghiti, E .V. Rusu, and I. M. Tiginyanu, Nanotechnology 19, 215714, (2008).
[15] A. N. Redkin, Z. I. Makovei, A. N. Gruzintsev, S. V. Dubonos, and E. E. Yakimov, Inorg. Mater. 43, 253, (2007).
[16] O. Lupan, G. A. Emelchenko, V. V. Ursaki, G. Chai, A. N. Redkin, A. N. Gruzintsev, I. M. Tiginyanu, L. Chow, L.K. Ono, B. R. Cuenya, H. Heinrich, and E.E. Yakimov, Mater. Res. Bull. 45, 1026, (2010).
[17] A. Ennaoui , M. Weber, R. Scheer, and H.J. Lewerenz, Sol. Energy Mater. Sol. Cells 54, 277, (1998).
[18] M. A. Zimmler, F. Capasso, S. Muller, and C. Ronning, Semicond. Sci. Technol. 25, 024001, (2010).
[19] R. Hauschild, and H. Kalt, Appl. Phys. Lett. 89, 123107, (2006).
[20] V. V. Ursaki, V. V. Zalamai, A. Burlacu, J. Fallert, C. Klingshirn, H. Kalt, G.A. Emelchenko, A. N. Redkin, A. N. Gruzintsev, E. V. Rusu, and I. M. Tiginyanu, Phys. D: Appl. Phys. 42, 095106, (2009).
[21] V. V. Ursaki, V. V. Zalamai, A. Burlacu, C. Klingshirn, E. Monaico, and I. M. Tiginyanu, Semicond. Sci. Technol. 24, 085017, (2009).

[22] O. Lupan, G. A. Emelchenko, V. V. Ursaki, G. Chai, A. N. Redkin, A. N. Gruzintsev, I. M. Tiginyanu, L. Chow, L. K. Ono, B. Roldan Cuenya, H. Heinrich, and E. E. Yakimov, Mater. Res. Bull. 45, 1026, (2010).
[23] B. K. Meyer, H. Alves, D. M. Hofmann, W. Kriegseis, D. Forster, F. Bertram, J. Christen, A. Hoffmann, M. Strasburg, M. Dworzak, U. Haboeck, and A.V. Rodina, Phys. Status Solidi (b) 241, 231 (2004).
[24] T. N. Morgan, Phys. Rev. 139, A343 (1965).
[25] V. V. Ursaki, I. M. Tiginyanu, V. V. Zalamai, E. V. Rusu, G. A. Emelchenko, V. M. Masalov, and E. N. Samarov, Phys. Rev. B, 70, 155204 (2004).
[26] V.V. Zalamai, V.V. Ursaki, E. Rusu, P. Arabadji, I.M. Tiginyanu, and L. Sirbu, Appl. Phys. Lett, 84, 5168, (2004).